Simulation of wavelength selection using ZnO nanowires array

Lijie Li[1*], Yan Zhang[2]

[1]Multidisciplinary Nanotechnology Centre, College of Engineering, Swansea University, Swansea, UK, SA2 8PP

[2]School of Physical Electronics, University of Electronic Science and Technology of China

**Corresponding emails: l.li@swansea.ac.uk*

Abstract: A new nanometer sized optical device dividing a beam of multi-wavelength light into constituent spectral wavelengths based on ZnO nanowires arrays has been presented, inspired by the diameter dependent energy bandgap of the nanowires. The theoretical validations based on the quantum optics theory have been conducted. It is shown from the simulation results that the output optical spectrum changes upon the energy bandgap of the material, which is determined by the diameter of the wire. The intensity of the optical spectrum is modeled depending on the charge density of the material. Potential applications of the proposed device on pressure sensitive imaging are discussed.

Keywords: Micro-optical devices, Subwavelength structures, nanostructures, wavelength-selection.

Introduction:

Nanotechnology has been experiencing explosive development in the last decade, on which many innovative electrical and optical devices are based. Recent advancement on zinc oxide (ZnO) nanostructures has been immense, evidenced by variety of research activities of applying them in energy harvesting [1], sensors [2 3], electronic and optical devices [4 5 6]. Inspired by the piezoelectric induced optical intensity enhancement on the ZnO nanowires [7], and energy bandgap variation depending on the diameter of the wires and their mechanical strain [8], we structure a new optical device based on ZnO nanowires arrays. Schematically shown in the Figure 1, the nanowires with graded diameters are arranged on a transparent substrate. Those nanowires with different diameters have different corresponding bandgaps, which split the incident multi-wavelength light into light waves with constituent wavelengths. The key feature of this approach is that, unlike other wavelength selection devices approaches where the wavelength of the light limits the size of the devices, the approach presented within this study uses output light from the device which is generated by the emission stimulated by electrons transiting from higher energy bands into lower energy bands, which is essentially the process of photon-electron-photon interaction process. Therefore, its behaviour is not governed by the dispersion of the optical waves, and is almost independent on the device dimensions. The new nanometer sized device can be used for designing miniaturized laser sources. Applications on the mechanical force sensitive imaging are also achievable as the device will have enhanced resolution due to the small dimension of nanowires.

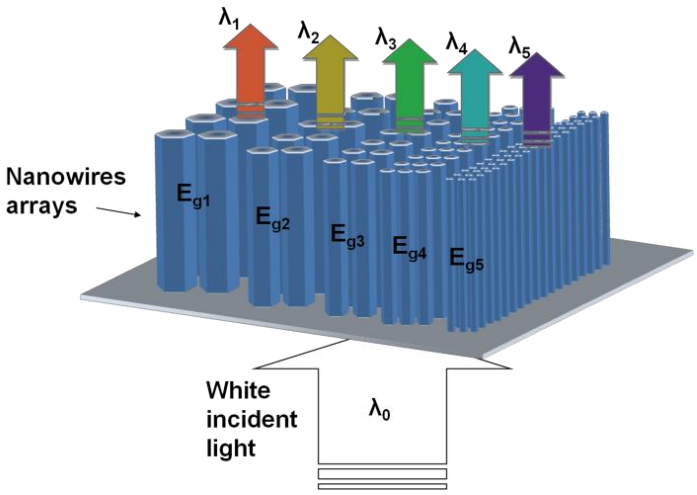

Figure 1 – schematic graph of the nanometer sized optical wavelength selector

Analysis and Results:

The luminescence of ZnO thin film and nanowires is usually having two maximums at a short wavelength and a long wavelength respectively [9]. The photoluminescence (PL) maximum at short wavelength is governed by the bandgap theory and is analyzed below underpinning the device concept. The PL maximum at long wavelength (green luminescence) has been reported for many reasons and has not been fully understood [10] [11] [12]. Experiments and discussions on the green luminescence explained that it is generated from the impurities and defects [9]. We ignore the green contributions as it is not determined by the bandgap of the ZnO itself and can be filtered out using substrate technology. The absorption of a wide range of optical spectrum by ZnO thin film is worth to study as the device concept is based on the absorption of incident light energy stimulating electrons migrating from higher states of the conduction band to lower states of the valence band emitting photons. The transmission of a beam of light through a ZnO film can be analyzed using classic optical theory from the wavelength dependent refractive of ZnO. The main equation expressing the transmitted amplitude is [13]

$$T_p = \frac{t_1 t_2 \exp(-i\delta)}{1 + r_1 r_2 \exp(-2i\delta)}$$

$$t_1 = \frac{2n_0}{n_0 + n_r(\lambda)}, \quad t_2 = \frac{2n_r(\lambda)}{n_r(\lambda) + n_0}, \quad r_1 = \frac{n_0 - n_r(\lambda)}{n_0 + n_r(\lambda)}, \quad r_2 = \frac{n_r(\lambda) - n_0}{n_r(\lambda) + n_0} \tag{1}$$

$$\delta = \frac{2\pi}{\lambda} n_r(\lambda) d \cos\varphi$$

where d denotes the thickness of the ZnO film, φ represents the incident angle of the light. $n_r(\lambda)$ represents the refractive index of the ZnO at wavelength λ. Sweeping wavelength of the input light from 300 nm to 1000 nm, transmission coefficient has been obtained as shown in the Figure 2. It is seen that the T-λ curve is a shape of high pass filter, indicating that light with long wavelengths passes through the material, and short wavelengths are absorbed by ZnO. This was experimentally reported in [14]. Note that the excitonic emission is possible for ZnO at room temperature as the exciton binding energy for ZnO is around 60 meV [15], which is much larger than the thermal energy k_BT at room temperature (~25 meV), which will cause an emission peak

at a longer wavelength, also known as a redshift [16]. However for this case, as the light absorption at long wavelengths is poor (Figure 2), we only consider the photoluminescence generated from the free electrons and holes.

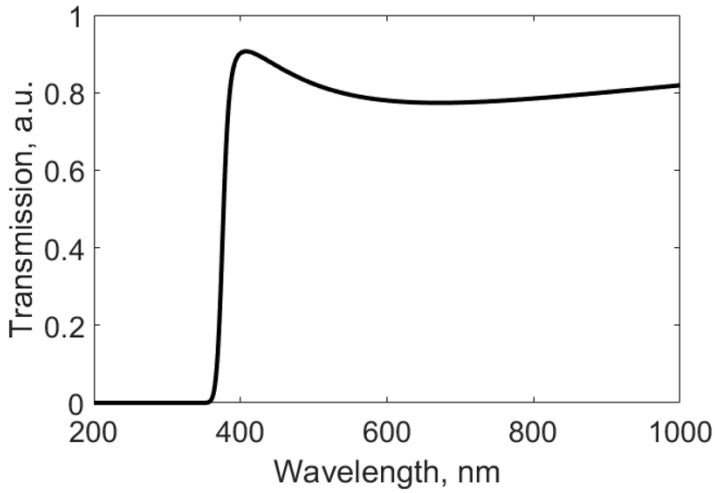

Figure 2 – calculated light transmission vs. wavelength. The thickness of the ZnO material is assumed to be 100 nm.

In order to demonstrate the beam filtering concept, the analysis of size dependent bandgap is presented first of all. Starting from an ultra-small dimension, such as the diameter of the nanowire less than 20 nm, quantum confinement effect will play the main role on the energy band structure. The conduction band minimum increases by ΔE_{quan} and the valence band maximum decreases attributed to electrons energy quantization. The energy bandgap of the nanowire E_g^{NW} can be approximately written as [17]

$$E_g^{NW} \cong E_g^{bulk} + \frac{\hbar^2 \pi^2}{2er^2}\left(\frac{1}{m_e} + \frac{1}{m_h}\right) - \frac{1.8e^2}{2\pi\varepsilon\varepsilon_0 d} \qquad (2)$$

where E_g^{bulk} is the bulk energy bandgap, d is the diameter of the nanowire, r denotes the radius of the nanowire, m_e is the effective mass of the electrons, and m_h is the effective mass of the holes. e denotes single electron charge, $\hbar$ is the reduced Planck constant, ε and ε_0 are relative permittivity and vacuum permittivity respectively. Equation (2) can be used for calculating the bandgap for nanowires with diameters less than 20 nm. The calculated E_g^{NW} for E_g^{bulk} = 3.35 eV, m_e = 0.2 m_0, m_h = 0.55 m_0, m_0 = 9.1 x 10^{-31} Kg, ε = 3.7 is shown in Figure 3 (red section of the curve). As the nanowire diameter D is larger than 50 nm, the quantum confinement effect diminishes, instead the surface effect dominates. The surface effect is caused by the atoms bonds shortening on the surface of the wire [18]. As the valence band maximum is predominately determined by the surface atoms [8], similar surface effect has been exhibited for TiO_2 nanowires and explained in [19], which will be lifted up a little depending on the degree of the surface effect (shown in the insert schematic graph of the Figure 3). Here E_h^{surf} is designated as the band shift of the valence band maximum subject to the surface effect, which is assumed when the diameter is 800 nm. As the diameter reduces, the bandgap increases, which can be regarded as the increase of the conduction band minimum ΔE_{surf}. The ΔE_{surf} is proportional to d^{-1}, which can be expressed as R_S/d. Rs is the parameter that can be extracted from experiments. The exact solution of the E_g^{NW} considering

the surface effect has to be solved by the First Principle method [20] [21]. Here an analytical approximation can be written as the function of the R_S and the diameter d. The expression of the E_g^{NW} is

$$E_g^{NW} \cong E_g^{bulk} - E_h^{surf} + R_s \frac{1}{d} \qquad (3)$$

E_g^{NW} can be smaller than bulk Eg because of the consideration of E_h^{surf}. The values of the E_h^{surf} and Rs have to be extracted by fitting the experimental data. R_s was extracted from Figure 3a of the reference [8]. Data of Figure 3a in the reference [8] was read when the strain equals 0, and was inserted to equation (3) to have a series of polynomial equations to obtain R_s. According to the reference [8], the best fitting can be achieved by designating the E_h^{surf} and Rs to 130 meV and 5.85 x 10^{-9} eV•m respectively. The calculated relation between E_g^{NW} and d is shown in Figure 3 using both the Quantum Dot (QD) approximation and the surface effect model. Extracted data of the experiments from reference [8] is also shown for comparison.

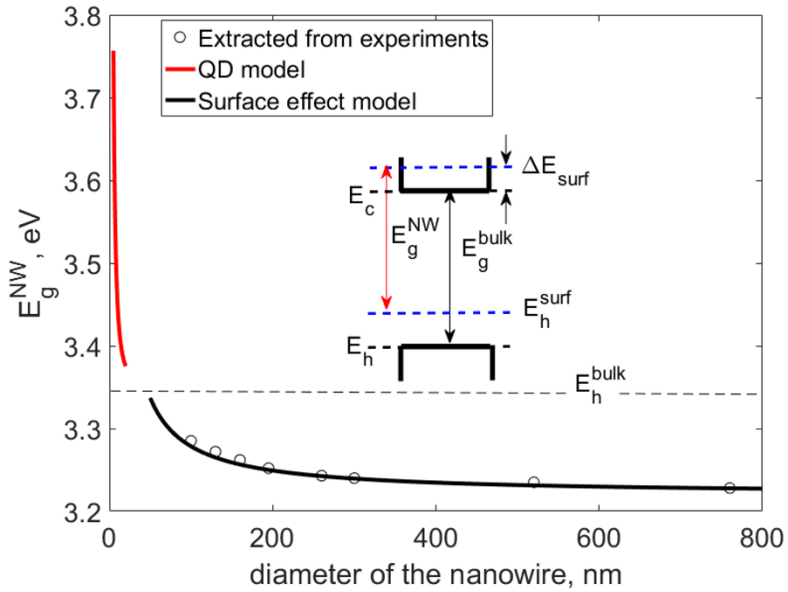

Figure 3 – calculated E_g^{NW} as functions of nanowire diameter d using quantum dot approximation and the surface effect model. Insert is the schematic of bandgap diagram.

Next we will find out how the bandgap influences the stimulated emission, which can be addressed using quantum mechanics theory. Incident light can be treated as an incident electromagnetic wave $A(r,t) = A_0 \cos(q \cdot r - \omega t)$, where the wave vector $q = \frac{\omega n_r}{c}$, n_r is the refractive index of the media, c is the speed of incident light and ω is the angular frequency of the plane wave. The stimulated emission occurs when an electron transits from a high energy state (a state in conduction band) to a low energy state (a state in valence band). The transition rate from the initial state in the conduction band to a final state in the valence band in the presence of electromagnetic radiation is given by Fermi's golden rule. The stimulated emission rate is given by

$$R = \frac{2\pi}{\hbar} \left| \langle \psi_2 | H' | \psi_1 \rangle \right|^2 \delta(E_c - E_v - \hbar\omega) \qquad (4)$$

where ψ_1 and ψ_2 are the initial and final wave function of the electron respectively, *H'* is the perturbation Hamiltonian $H' = \frac{e}{2m} A_0 e^{iq \cdot r} \cdot q$. E_c and E_v represent conduction band minimum and valence band maximum respectively. The transition rate is determined by the strength of the coupling between initial and final states, and the number of ways the transition can occur, i.e. the density of states. Assume that a number of transitions happening per unit volume of material per second, the total transition rate is

$$E_{St} = \frac{2}{V}\left(\sum_k R\right) f_e f_h \qquad (5)$$

where f_e and f_h are Fermi-Dirac distribution functions of electrons and holes in the material respectively ($\frac{1}{e^{(E-\mu)/k_B T} + 1}$). *V* represents the volume of the material, and *R* is the stimulated emission rate expressed in the equation (4). After several mathematic derivation procedures such as the separation of fast varying and slow varying exponents in the integrand and breaking up the integral over the entire crystal into integrals over all the primitive cells. The following equation is arrived

$$\frac{2}{V}\sum_k R = \frac{2\pi}{\hbar}\left(\frac{qA_0}{2m}\right)^2 \left\langle \left| \hat{\bar{p}}_{cv} \cdot \hat{n} \right|^2 \right\rangle \times 2\int \frac{d^3k}{(2\pi)^3} \delta(E_c - E_v - \hbar\omega) \qquad (6)$$

The $\left| \hat{\bar{p}}_{cv} \cdot \hat{n} \right|^2$ is squared momentum matrix element depending on the electron wavevector *k* and also the polarization direction of the incident electromagnetic wave. In most of III-V and II-IV semiconductors, the average value of the momentum matrix element can be treated as constant [22], expressed in terms of the Kane energy E_p, as $\left\langle \left| \hat{\bar{p}}_{cv} \cdot \hat{n} \right|^2 \right\rangle = \frac{mE_p}{6}$. The E_p for most of II-IV and III-V semiconductors can be sourced from references [23] [24]. $\int \frac{d^3k}{(2\pi)^3} \delta(E_c - E_v - \hbar\omega)$ is the density of states *g(E)* in three-dimensions. d^3k is the volume element of **k**-space, $d^3k = dk_x \cdot dk_y \cdot dk_z$. Density of states (DOS) is defined as the number of states in a conductor per unit energy. We use the DOS for electrons confined in 3D (also known as 0D DOS) for this case. Using 0D DOS is to avoid the infinity value at E_0=0 of the 1D DOS ($DOS_{1D} \propto 1/\sqrt{E}$). The DOS for electrons confined in 3D is expressed as

$$g(E) = \frac{2}{\pi} \frac{\hbar/2\tau}{(\hbar\omega - E_g)^2 + (\hbar/2\tau)^2} \qquad (7)$$

Equation (7) is known as the Lorentzian equation. The width of the Lorentzian at half its peak value (full width at half maximum, or FWHM) is $\hbar/\tau$. The coupling between the nanowire and adjacent contact can be described by the coupling energy $\Gamma = \hbar/\tau$ or the lifetime of the electron on the nanowire τ . The DOS of 1D quantum wire can be represented by the 0D DOS when the coupling energy Γ is small (Γ for ZnO nanowire could not be found, here Γ =20 meV for demonstration purpose). Stimulated emission using 3D confined density of states, E_{st} is given by

$$E_{st} = \frac{2\pi}{\hbar}\left(\frac{qA_0}{2m}\right)^2 \left\langle \left| \hat{\bar{p}}_{cv} \cdot \hat{n} \right|^2 \right\rangle \times \frac{2}{\pi} \frac{\Gamma/2}{(\hbar\omega - E_g)^2 + (\Gamma/2)^2} f_e f_h \qquad (8)$$

Re-arrange equations (8), let $M = \left\langle \left| \vec{p}_{cv} \cdot \vec{n} \right|^2 \right\rangle$, and substitute q by $(\omega \cdot n_r)/c$, one can get

$$E_{st} = \frac{A_0^2 M}{m^2 \hbar^3 c^2} (\hbar\omega)^2 n_r^2 \frac{\Gamma/2}{(\hbar\omega - E_g)^2 + (\Gamma/2)^2} f_e f_h \tag{9}$$

Hence the scaled stimulated emissions ($E_{st}^{'} = \frac{E_{St} m^2 \hbar^3 c^2}{A_0^2 M}$) is given by

$$E_{st}^{'} = (\hbar\omega)^2 n_r^2(\omega) \frac{\Gamma/2}{(\hbar\omega - E_g)^2 + (\Gamma/2)^2} f_e f_h \tag{10}$$

where $\hbar\omega$ is the photon energy E_p. It is seen that the stimulated emission is proportional to the incident photon energy, refractive index, DOS and Fermi distributions of electrons and holes. Numerical solution to this equation is conducted. Dispersion in the refractive index ($dn_r/d\lambda$) is considered in the quantum mechanics simulation. The chemical potential for a number of electrons and holes per unit volume at certain temperatures is required to calculate the f_e and f_h. To calculate the chemical potential for electrons or holes, an initial value of the chemical potential is estimated. The maximum possible value of the chemical potential is given by the Fermi energy $\mu_{\max} = E_F = \frac{\hbar^2 k_F^2}{2m}$, where $k_F = (3\pi^2 n_c)^{1/3}$, n_c is the carrier density. The minimum possible value of the chemical potential is given by the high-temperature limit ($T \to \infty$). In this limit, the Fermi-Dirac distribution becomes Boltzmann distribution

$$f(E)|_{T\to\infty} = \frac{1}{e^{(E-\mu)/k_B T} + 1}\bigg|_{T\to\infty} = e^{(\mu - E)/k_B T} \tag{11}$$

A three dimensional electron gas in this high temperature limit has the chemical potential

$$\mu_{\min} = k_B T \ln\left(\frac{n}{2} \left(\frac{2\pi\hbar^2}{mk_B T} \right)^{3/2} \right) \tag{12}$$

Carrier density n_c can be calculated using an integral over energy

$$n = \frac{1}{2\pi^2} \left(\frac{2m}{\hbar^2} \right)^{3/2} \int_{E_{\min}=0}^{E_{\max}=\infty} E^{1/2} \frac{1}{e^{(E-\mu)/k_B T} + 1} dE \tag{13}$$

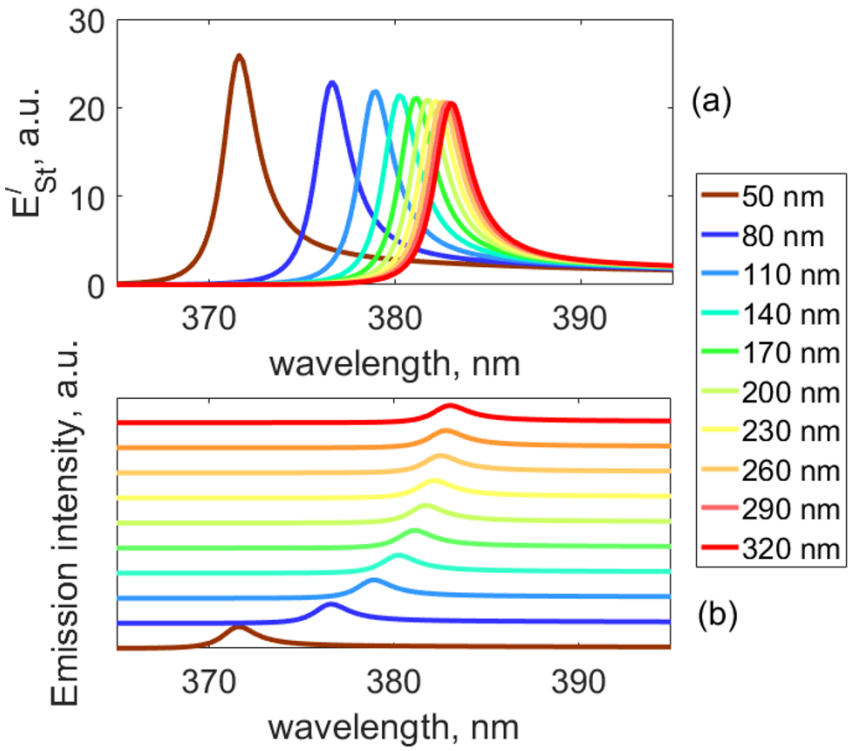

Figure 4 – Simulation results using quantum mechanics theory on the nanometer sized prism. (a) results show filtering effect. (b) a clearer view of the results, especially for nanowires diameters from 170 nm to 320 nm.

A computer iteration process is used to calculate the chemical potential for both electrons and holes respectively (μ_e, μ_h). The calculated chemical potentials for electrons and holes are then used in equation (10) to calculate the stimulated emission rate. The bandgap of ZnO nanowire varies with its size and force induced strains [8]. In the calculation, we first evaluate the beam filtering effect by passing a beam of white light consisting of a range of wavelengths varying from 360 nm to 400 nm through arrays of nanowires with diameters increasing from 50 nm to 320 nm with a step size of 30 nm. Bulk energy bandgap of 3.35 eV is taken into the calculation. The relation between the diameter and the bandgap is used according to the equation (3). Other parameters used in the equation (3) are the same as calculating the results in Figure 3. Based on primarily the equation (10), results in Figure 4 display the scaled stimulated emissions for arrays of nanowires with different diameters. It is worth noting that the calculated shapes match with observations from previous experiments [25] [26] [27]. Small diameter wires having wider bandgaps emit higher energy waves with narrower wavelengths. It also shows that the shift of the wavelength in connection to the linearly increased diameters is not linear. Nanowires with diameters larger than 380 nm will not have much difference in emitted wavelength, this can be seen clearly in the Figure 4b.

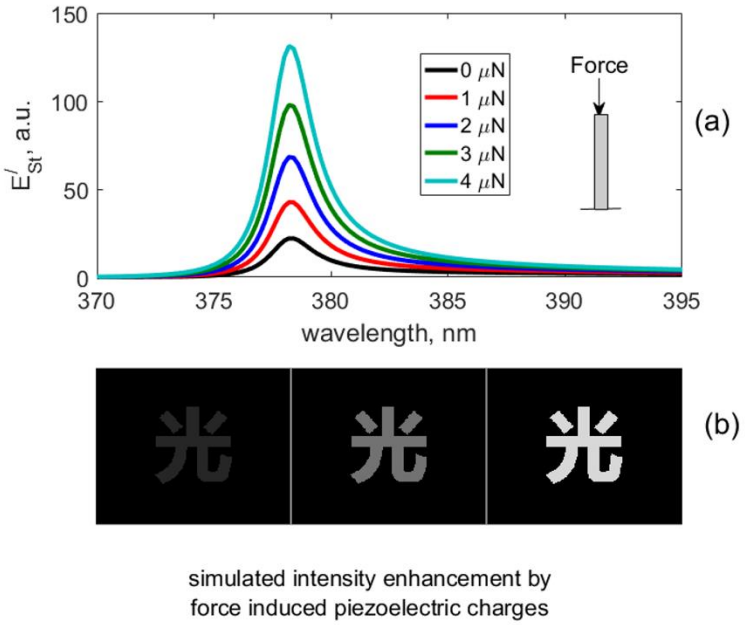

Figure 5 – The intensity of the stimulated emission can be enhanced by external applied force to a piezoelectric nanowires arrays. (a) calculated emission under different forces. (b) demonstration of the image enhancement by the mechanical force.

The intensity of the stimulated emission can also be adjusted by changing the carrier density inside the semiconductor nanowires. Known as a piezoelectric and semiconducting material, a ZnO nanowire can produce electrical charges subject to external applied mechanical forces. Interaction between electrical and mechanical properties of the piezoelectric medium can be expressed as

$$\begin{aligned} S &= s^E T + dE \\ D &= dT + \varepsilon^T E \end{aligned} \qquad (14)$$

where S, T, E, D are strain, stress, electrical filed strength, and dielectric displacement respectively. s, d, ε are mechanical compliance, piezoelectric constant and permittivity, where the superscripts to the symbols denote the quantity kept constant under boundary conditions. For this case, the electrical circuit connecting two ends of the nanowire is open, assuming there is no external electrical field the equation (14) is simplified to $D = dT$. The force is applied along the c-axis of the nanowire, the induced electrical charge $Q = d_{33}F$, where F is the force applied, d_{33} is the piezoelectric constant defined as the induced polarization per unit applied stress in direction 3 (c –axis). For the ZnO nanowire, piezoelectric constant d_{33} = 5.43 x 10^{-12} C/N [28]. It is assumed that the applied force ranges from 0 to 4 μN, considering the dimension of the nanowire as 50 nm in diameter, 100 nm in length, the calculated increment of the carrier density is up to 1.09 x 10^{24} m^{-3}. This increment will be taken into the equation (10) to calculate the stimulated emission. Results (in Figure 5) show that as the increase of the applied axial force, nanowires emit much more intensified light. This phenomenon can be useful to design force dependent imaging device. Figure 5b demonstrates that the intensity of an image can be enhanced by increasing the axial force. To further clarify, spontaneous emission is the phenomenon where an electron spontaneously decays from an excited state to a lower state emitting a photon. Stimulated emission is when a photon interacts with an electron in the excited state, which drops to a lower state emitting a photon with the same properties (frequency, direction) as the incident photon. The stimulated emission is

the key for this concept. The device can be fabricated through the hydrothermal method, which is sketched as follows. The fabrication steps will start with selectively coating of a stripe of ZnO seed layer; then a second stripe of seed layer will be coated with slightly increased thickness. More stripes of seed layers will be coated with increasing thicknesses until reaching to the number of required wavelengths. Finally, the synthesis of nanowires will be conducted hydrothermally. This approach is based on previous experiments showing that the average diameter of nanowires is increased from 50 to 130 nm when the seed layer thickness is changed from 20 to 1000 nm [29].

Conclusion: In conclusion, a new nanometer sized optical wavelength selector based on ZnO nanowires arrays has been proposed and simulated based on quantum optics theory. The model has validated the filtering effect using nanowires arrays with various diameters. The emission can be enhanced by increasing the carrier density in the material, which can be realized from charges generation of piezoelectric effect. Theoretical modeling of the force induced intensity enhancement has been conducted.

Acknowledgement:

LL very much appreciates Professor Deepak Uttamchandani at University of Strathclyde for his conceptual contribution, fruitful advice, and encouragement on this work.

Author information

The authors declare no competing financial interest.

References

1. Z. L. Wang and J. Song, Science **312** (5771), 242-246 (2006).
2. Q. Wan, Q. H. Li, Y. J. Chen, T. H. Wang, X. L. He, J. P. Li and C. L. Lin, Applied Physics Letters **84** (18), 3654-3656 (2004).
3. T. Y. Chen, H. I. Chen, C. S. Hsu, C. C. Huang, J. S. Wu, P. C. Chou and W. C. Liu, Sensors and Actuators B-Chemical **221**, 491-498 (2015).
4. L. Li, Applied Physics Letters **103** (23) (2013).
5. M. H. Huang, S. Mao, H. Feick, H. Q. Yan, Y. Y. Wu, H. Kind, E. Weber, R. Russo and P. D. Yang, Science **292** (5523), 1897-1899 (2001).
6. P. D. Yang, H. Q. Yan, S. Mao, R. Russo, J. Johnson, R. Saykally, N. Morris, J. Pham, R. R. He and H. J. Choi, Advanced Functional Materials **12** (5), 323-331 (2002).
7. C. Pan, L. Dong, G. Zhu, S. Niu, R. Yu, Q. Yang, Y. Liu and Z. L. Wang, Nat Photon **7** (9), 752-758 (2013).
8. B. Wei, K. Zheng, Y. Ji, Y. Zhang, Z. Zhang and X. Han, Nano Letters **12** (9), 4595-4599 (2012).
9. P. A. Rodnyi and I. V. Khodyuk, Optics and Spectroscopy **111** (5), 776-785 (2011).
10. F. Fabbri, M. Villani, A. Catellani, A. Calzolari, G. Cicero, D. Calestani, G. Calestani, A. Zappettini, B. Dierre, T. Sekiguchi and G. Salviati, Scientific Reports **4**, 5158 (2014).
11. J. Čížek, J. Valenta, P. Hruška, O. Melikhova, I. Procházka, M. Novotný and J. Bulíř, Applied Physics Letters **106** (25), 251902 (2015).
12. W. Maenhout-Van Der Vorst and F. van Craeynest, physica status solidi (b) **9** (3), 749-752 (1965).
13. O. S. Heavens, *Optical Properties of Thin Solid Films*. (Dover Publications, New York, 1965).
14. R. C. Rai, Journal of Applied Physics **113** (15), 153508 (2013).
15. W. Zhong Lin, Journal of Physics: Condensed Matter **16** (25), R829 (2004).
16. C. H. Ahn, S. K. Mohanta, N. E. Lee and H. K. Cho, Applied Physics Letters **94** (26), 261904 (2009).

17. K. F. Lin, H. M. Cheng, H. C. Hsu, L. J. Lin and W. F. Hsieh, Chemical Physics Letters **409** (4-6), 208-211 (2005).
18. M.-R. He, R. Yu and J. Zhu, Nano Letters **12** (2), 704-708 (2012).
19. D. B. Migas, A. B. Filonov, V. E. Borisenko and N. V. Skorodumova, Physical Chemistry Chemical Physics **16** (20), 9479-9489 (2014).
20. R. Agrawal and H. D. Espinosa, Nano Letters **11** (2), 786-790 (2011).
21. Q. Jingshan, S. Daning and J. Jianming, Nanotechnology **19** (43), 435707 (2008).
22. G. Jacopin, L. Rigutti, A. D. L. Bugallo, F. H. Julien, C. Baratto, E. Comini, M. Ferroni and M. Tchernycheva, Nanoscale Research Letters **6** (2011).
23. V. A. Fonoberov and A. A. Balandin, Journal of Nanoelectronics and Optoelectronics **1** (1), 19-38 (2006).
24. P. Lawaetz, Physical Review B **4** (10), 3460-& (1971).
25. C.-H. Chen, S.-J. Chang, S.-P. Chang, M.-J. Li, I.-C. Chen, T.-J. Hsueh and C.-L. Hsu, Applied Physics Letters **95** (22), 223101 (2009).
26. G. Signorello, S. Karg, M. T. Bjork, B. Gotsmann and H. Riel, Nano Letters **13** (3), 917-924 (2013).
27. C. Baratto, R. Kumar, E. Comini, G. Faglia and G. Sberveglieri, Optics Express **23** (15), 18937-18942 (2015).
28. W. Han, Y. Zhou, Y. Zhang, C.-Y. Chen, L. Lin, X. Wang, S. Wang and Z. L. Wang, Acs Nano **6** (5), 3760-3766 (2012).
29. L.-W. Ji, S.-M. Peng, J.-S. Wu, W.-S. Shih, C.-Z. Wu and I. T. Tang, Journal of Physics and Chemistry of Solids **70** (10), 1359-1362 (2009).